J Therm Anal Calorim (2014) 118:349–357
DOI 10.1007/s10973-014-3965-2

The influence of silicone shell on double-layered microcapsules in intumescent flame-retardant natural rubber composites

Na Wang · Yuhu Wu · Long Mi · Jing Zhang · Xuri Li · Qinghong Fang

Received: 19 March 2014 / Accepted: 14 June 2014 / Published online: 10 September 2014

Abstract Double-shell co-microencapsulated ammonium polyphosphate and mesoporous MCM-41 (M(A&M)) were prepared by using melamine–formaldehyde resin and organic silicon in situ polymerization. The structure of the microcapsules was characterized by Fourier-transform infrared spectroscopy, particle size analysis, and scanning electron microscopy. In particular, the influence of basic properties of flame-retardant natural rubber , such as flame-retardant and mechanical property, was investigated with the limiting oxygen index, UL-94 test, thermogravimetric analysis, tensile test, and rubber process analyzer (RPA). Due to the presence of organic silicone shell, the NR/M(A&M) composites had much better flame-retardant and mechanical properties than other flame-retardant natural rubber (NR) composites. The limited oxygen index value of the NR/M(A&M) composite reached the maximum, and the UL-94 ratings were increased to V-0. Furthermore, M(A&M) showed better compatibility in NR system by the RPA. The occurrence of a synergistic effect between MCM-41 and intumescent flame-retardant in the NR composites was proved. As a result, the thermal stability and flame retardancy of NR were enhanced.

Keywords Double-shell co-microencapsulated · Organic silicon · Synergism · Mesoporous MCM-41 · Intumescent flame retardant · Natural rubber

N. Wang (✉) · Y. Wu · L. Mi · J. Zhang · X. Li · Q. Fang
College of Materials Science and Engineering, Shenyang University of Chemical Technology, Shenyang 110142, China
e-mail: iamwangna@sina.com

N. Wang
College of Materials Science and Chemical Engineering, Harbin Engineering University, Harbin 150001, China

Introduction

Natural rubber (NR) has many unique advantages over competitive synthetic rubbers by virtue of its unique combination of physico-mechanical properties. And its latitude of application is being widened day by day, by the judicious design and compounding of formulations for specific applications. However, despite a number of superior qualities, its inherent high flammability prevents NR from being used in some highly demanding applications such as coal mine convey or belts, power cables, aircraft tire treads, and so on [1–3].

Because of the potential demand of flame-retardant natural rubber (FRNR) for diverse applications, FRNR has been a hot research topic. Among the various approaches to confer flame retardancy to NR, intumescent flame retardants (IFR) with little smoke release and low toxicity are preferable additives in NR compared with traditional flame retardants containing phosphorus or halogen [4, 5]. A widely used IFR system is a mixture of ammonium polyphosphate (APP), pentaerythritol (PER), and melamine (MEL). Synergism has been found between IFR and MCM-41 or SBA−15 in PP composites (PP-IFR) in our previous work [6]. Results show that mesoporous silica MCM-41 and SBA−15 exert the effective synergistic effect found in intumescent flame-retardant systems of PP to obtain good flame retardancy and satisfactory mechanical properties. But due to its high water solubility and low compatibility with matrix material, the IFR system is not durable, and microencapsulation of IFR system has been regarded as an effective strategy. Chen, Xilei et al. [7, 8] successfully microencapsulated APP with polyurethane (PU), urea-melamine-formaldehyde (UMF) resin, and PVA-MEL-formaldehyde resin shell. To improve the FR properties of composites, microencapsulated ammonium polyphosphate

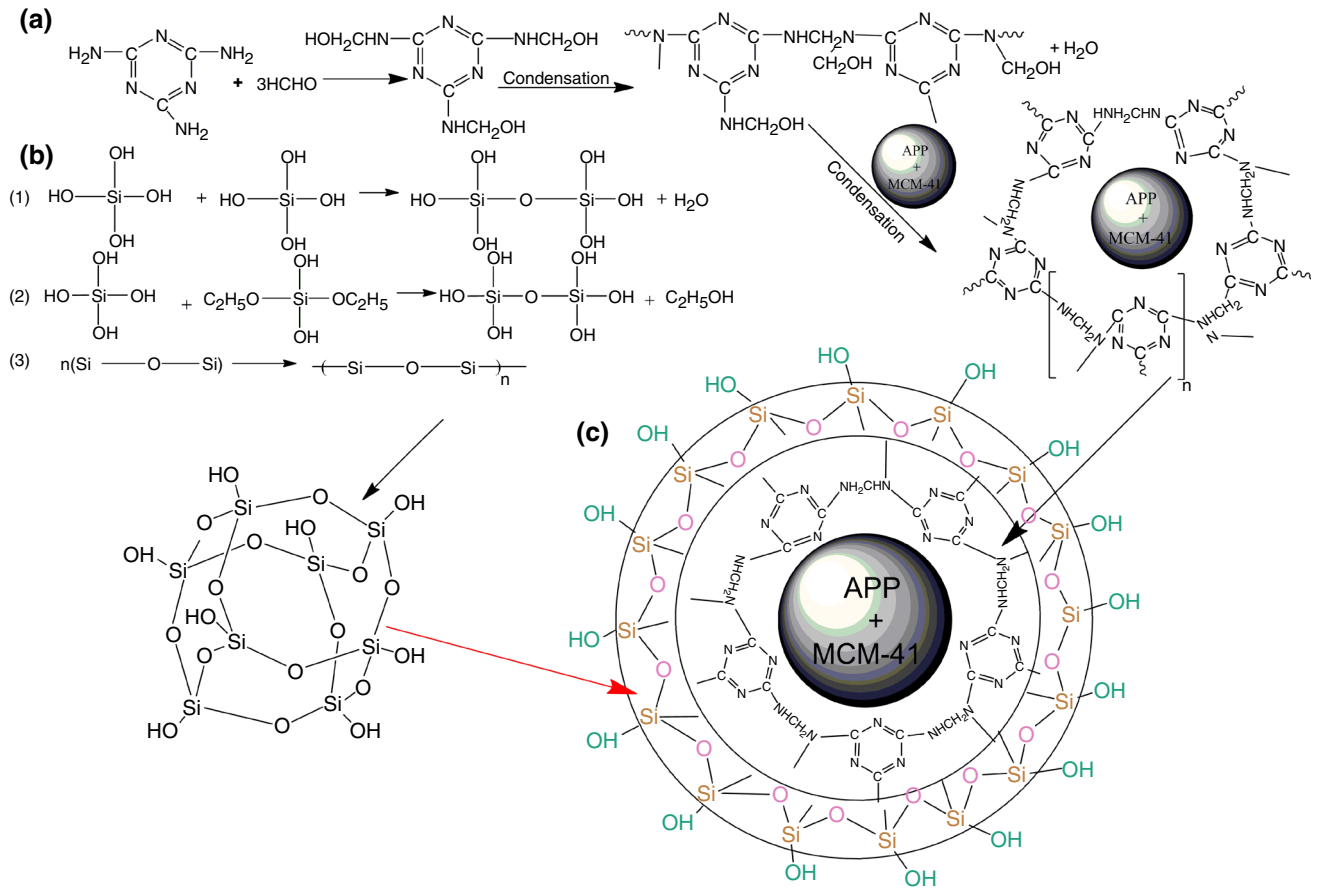

Fig. 1 **a** Schematic of the double-shell MC(A&M), **b** schematic of the shell formation process of the MF, **c** schematic of the shell formation process of the OS

with melamine–formaldehyde resin (MCAPP) prepared by in situ polymerization that showed decreased water solubility and particle size, which was better than ammonium polyphosphate (APP), was used as additive to NR together with mesoporous silica MCM-41 as a synergistic agent to form IFR composite in our recent study [9]. However, the ideal mechanical and FR properties of NR composites cannot be achieved by the single-layered microencapsulation of IFR. And then, we studied the double-layered co-microencapsulated APP and MCM-41 fillers (M(A&M)) with MEL-formaldehyde (MF) resin and zinc borate (ZB) in intumescent flame-retardant natural rubber composites [10] to solve the problem mentioned. As the outer shell is made of inorganic ZB materials, the compatibility and material mechanical performance are still not ideal.

With the advantages of both the inorganic material and organic material, organic silica (OS) has a good application prospect. The chemical modification or functionalization of OS and attachment of the modified OS to PUs are of great interest owing to their improved properties and potential use in several different applications. This system with covalently anchored functional groups on the silica causes its surface to have specific attributes, such as a stereochemical configuration and binding sites that enhance compatibility with NR matrix which improves thermal stability [11–14].

In this paper, the double-shell co-microencapsulated APP and MCM-41 fillers M(A&M) with MEL-formaldehyde (MF) resin and OS (Fig. 1c) were prepared by in situ polymerization. The structure of the microcapsules was characterized by Fourier-transform infrared spectroscopy, particle size analysis, and scanning electron microscopy. In particular, the influence of basic properties of FRNR, such as flame-retardant and mechanical property, was investigated with the limiting oxygen index, UL 94 test, thermogravimetric analysis, tensile test, and rubber process analyzer (RPA).

Experimental

Materials

Natural rubber SMR-20 was provided by Petrochemical Co., Jilin. The commercial product APP (phase II, average degree of polymerization $n > 1000$, soluble fraction in

$H_2O < 0.5$ mass%) was supplied by Shifang Changfeng Chemical Co., Ltd., China. PER and MEL were supplied by Sinopharm Chemical Reagent Co., Ltd. The mixture of APP, PER, and MEL was set at a mass ratio of 3:1:1, at which the FR properties were the maximum [4]. Bis-(γ-triethoxysilylpropyl)-tetrasulfide (TESPT) was provided by Evonik Degussa Co. Ltd. Analytical-grade tetraethyl silicate, stearic acid, sulfur, and other chemicals were used as received.

Spherically shaped mesoporous MCM-41 particles with uniform diameters within the range of 80–100 nm were prepared in the laboratory following a previously described method [15]. Infrared analysis of the synthesized nanosized mesoporous MCM-41 particles has been reported in a previous work [16].

Preparation of microcapsules

Preparation of MF pre-polymer: 15 g of MEL, 34 g of 37 mass% formaldehyde solution, 0.3 g of Na_2CO_3, and 40.0 mL of deionized water were added to a three-necked bottle with a stirrer (230 rpm). The mixture was heated to 80 °C and kept at that temperature for 1 h. The MF pre-polymer solution was then prepared, and it was ready for microencapsulation of APP and MCM-41.

Preparation of single-shell microcapsules: a mixture of APP and MCM-41 (60 g) and 150 mL of ethanol were added to a three-neck bottle, under stirring (300 rpm, 20 min). Then, the MF pre-polymer solution, whose pH was adjusted to 5–6 with hydrochloric acid dilution. The resulting mixture was heated to 75 °C for 2 h. The condensation reaction mechanism of the MF is shown in Fig. 1a.

Preparation of double-shell microencapsules: tetraethyl silicate (40 g), anhydrous ethanol (40 g), and distilled water (80 g) were added to a three-necked bottle, and the pH of the mixture was adjusted to pH 2–3 with sulfuric acid. The resulting mixture was heated at 60 °C for 3 h with stirring (350 rpm). After the hydrolysis reaction of the tetraethyl silicate had taken place, the sol solution as encapsulation precursor was obtained. The single-wall microcapsules were added into mixture solution with stirring (400 rpm, 2 h), and the temperature of the sol solution was controlled at 30 °C using a constant temperature bath. The condensation reaction mechanism and hydrolysis reaction mechanism of the tetraethyl silicate onto the surface of single-wall microcapsules are shown in Fig. 1b.

Preparation of FRNR composites

Flame-retardant natural rubber composites were mixed with the change of the amount of IFR agents and rubber compounds into NR according to the recipe in Table 1 by a laboratory two-roll mill. The components of NR compounds included stearic acid, PER, MEL, TESPT, carbon soot, zinc oxide, sulfur, age inhibitor 4010, electric insulating oil, accelerant CZ, and tetramethylthiuram disulfide, which had fixed values of 35, 13, 13, 5, 5,4, 1.2, 1, 1, 0.8, 0.35, (phr), respectively. All NR samples were vulcanized at 145 °C in a hot press for the optimum cure time t90 determined by a GT-M2000-A rheometer (GaoTie Limited Co., Taiwan). All specimens were then cut from the vulcanized sheets and conditioned at 20 °C for 24 h before testing.

Table 1 Formulation of FRNR composites

Sample	NR/phr	APP/phr	MCAPP/phr	MCM-41/phr	M(A&M)/phr
NR	100	/	/	/	/
NR/APP	100	40	/	/	/
NR/MCAPP	100	/	40	/	/
NR/M(A&M)	100	/	/	/	40(APP/MCM-41 39/1)
NR/MCAPP/MCM-41	100	/	39	1	/

Characterization

The infrared spectra of the microcapsules were obtained on a Nicolet MNGNA-IR 560 with 4 cm^{-1} resolution. Mean particle size and distribution of microcapsules were evaluated by a laser particle size analyzer (Rise-2008, Shandong, China). The SEM images of the microcapsules and NR composites were obtained with a scanning electron microscope JEOL JSM-6360LV. The specimens were previously coated with a conductive gold layer. The samples for testing the morphology of the burnt composites were prepared using burnt samples of oxygen index. Complete burning of the samples was ensured. LOI data were obtained at room temperature on an oxygen index instrument (JF-3) produced by Jiangning Analysis Instrument Company, China, according to ISO 4589−1984 standard. The dimensions of the specimens were $126 \times 6.5 \times 3$ mm^3. The vertical test was carried out on a CFZ-2 type instrument (Jiangning Analysis Instrument Company, China) according to the UL-94 test standard. The specimens used had dimensions of $126 \times 13 \times 3$ mm^3. Room-temperature tensile tests of the composites were conducted following GB/T528−1998 on an Instron 1211 testing machine at a crosshead speed of 500 mm min^{-1}. The thermal stability of the NR composites was examined by TG using a Perkin-Elmer TGA 7 thermal analyzer at a heating rate of 10 °C min^{-1}. Nitrogen was used as a carrier gas at a constant flow rate during analysis. Dynamic mechanical properties were measured

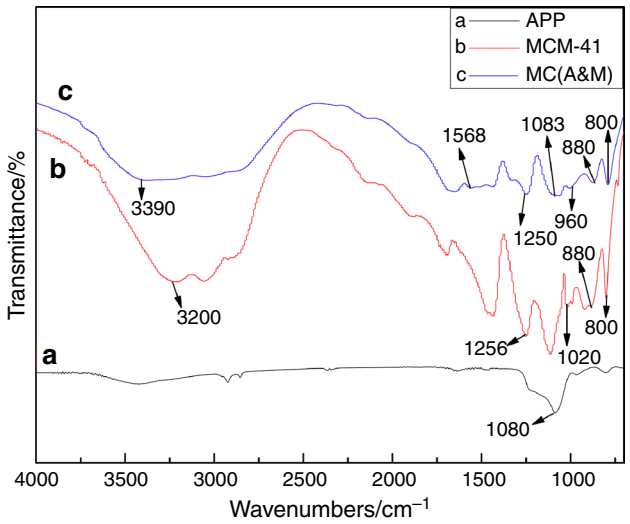

Fig. 2 FTIR spectra of APP, MCM-41 and MC(A&M)

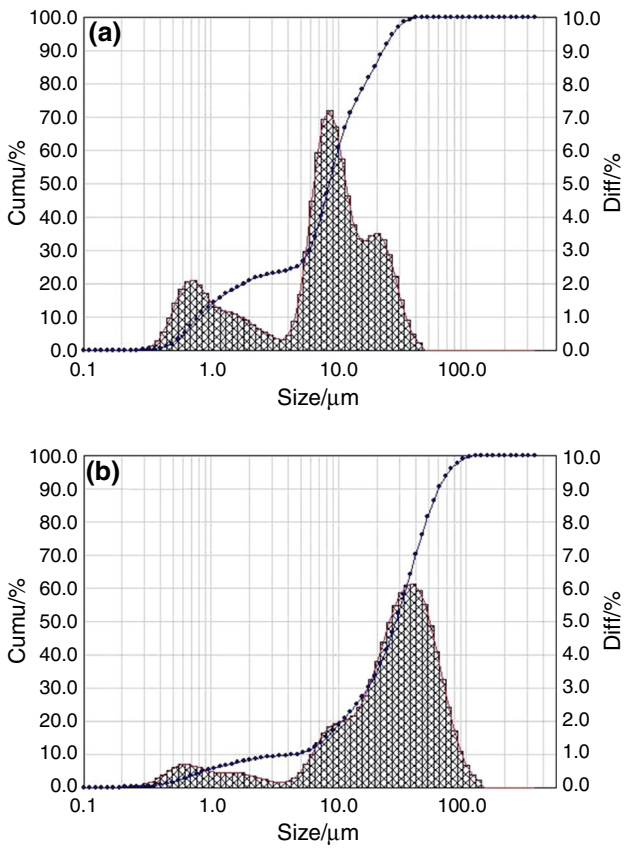

Fig. 3 Size distribution of APP (**a**) and M(A&M) (**b**)

with a dynamic mechanical thermal analyzer (DMTAV, Rheometrics Science Corp.). The dynamic storage modulus was determined at a frequency of 10 Hz and a heating rate of 3 °C min^{-1} from −100 to 100 °C. Curing was performed on Rubber Process Analyzer RPA-8000 (GaoTie Limited Co., Taiwan) at the temperature of 145 °C, frequency of 100 cpm, and strain amplitude of 0.5°. For strain sweep, the temperature was 60 °C, the frequency was 60 cpm, and the strain was between 1 and 100 %.

Results and discussion

Characterization of microcapsules

The FTIR spectra of APP and M(A&M) are shown in Fig. 2. Figure 2a shows the typical absorption peaks of APP at 3200 (N–H), 1256 (P = O), 1020 (symmetric vibration of PO_2), 880 (P–O asymmetric stretching vibration), and 800 cm^{-1} [17]. Figure 2b shows that the 1080 cm^{-1} band represented the asymmetric stretching vibration of Si–O–Si from MCM-41. As shown in Fig. 2c, the main absorption peaks appeared at 3390, 1568, 1250, 1083, 960, 800, and 463 cm^{-1}. The peaks at 1083, 798, and 463 cm^{-1} signify the bending vibration of the Si–O functional group, and the peak at 960 cm^{-1} is assigned to the Si–OH functional group [18]. The absorption at 1568 cm^{-1} is due to the ring vibration of MEL from MF resin. Consequently, the spectrum of M(A&M) reveals the characteristic bands of APP/MCM-41 and the well-defined absorption peaks of MF resin and OS.

Figure 3 shows the number-average particle size distribution of APP and M(A&M). Both APP and M(A&M) are in the size range of 0.1–120 μm, but the mean particle size of double-shell microcapsules increases to 28.05 μm compared to the 8.43 μm of APP. And Fig. 3 clearly shows that the particle size distributions of M(A&M) become more concentrated than APP without microencapsulated. Because of the narrow particle size distribution of M(A&M), it has better compatibility in NR than APP when blended with NR in this study, which expects for better flame retardancy and mechanical properties.

The surface morphologies of the APP and M(A&M) particles are shown in Fig. 4. The surface of APP particle is obviously very smooth. It is observed from the SEM micrographs that the presence of OS shell does affect the morphological makeup of the microparticles. M(A&M) is observed to have uneven surfaces that are likely due to the fact that the methylolation reaction in the synthesis of MF resin produced different addition products. A second step of polycondensation results in different degrees of polymerization of the inner layer MF resin to produce this phenomenon. Thus, double-layered microencapsulation is achieved. As expected, the functionalized organic group after crosslinking make the M(A&M) be incorporated into NR three-dimensioned network, which can enhance the dispersion of M(A&M) and the compatibility between NR matrix and M(A&M).

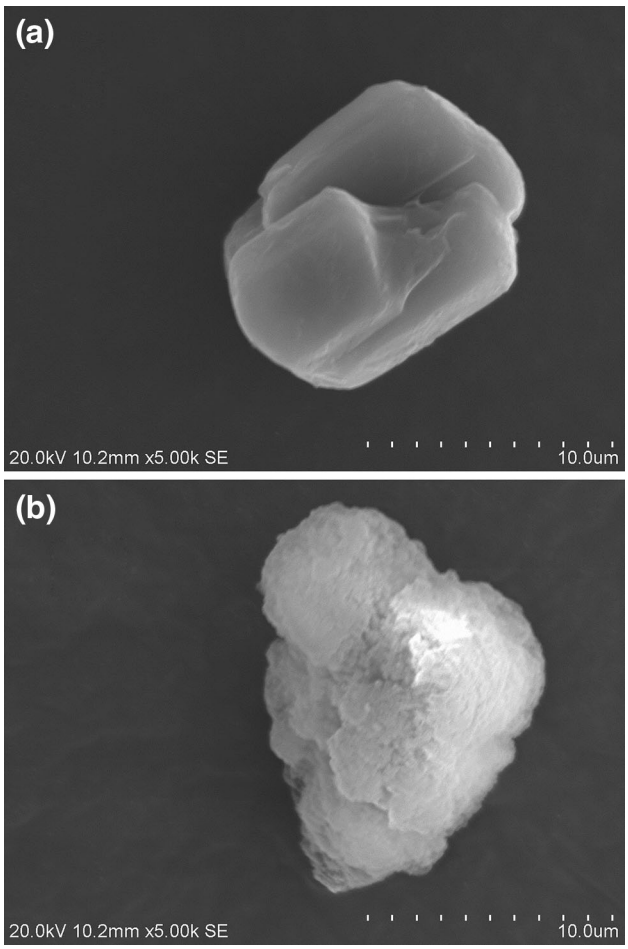

Fig. 4 SEM images of APP particles (**a**) and M(A&M) particles (**b**)

Table 2 Flame retardancy and mechanical property of flame-retardant NR composites

Flame-retardant composite	Flame retardancy		Mechanical property	
	LOI/%	UL-94	Tensile strength/MPa	Elongation at break/%
NR	16	No rating	22.25	452.6
NR/APP	26.2	No rating	6.62	276.6
NR/MCAPP	28.7	V-0	7.50	272.6
NR/M(A&M)	29.9	V-0	8.23	309.6
NR/MCAPP/MCM-41	29.2	V-0	7.68	348.2

Flame retardancy

LOI and UL-94 tests are widely used to determine the flammability of flame-retardant materials. From the experimental results shown in Table 2, NR is easily flammable polymeric material with a LOI value of 16, and it cannot pass UL-94 test. The improvements in flame retardancy of the vulcanizates at higher concentrations of M(A&M) are clear from the increase in value of LOI from 26.2 to 29.9 as given in Table 2. The experimental results of vertical burning rate show that the NR/M(A&M) systems give a V-0 rating. It can be clearly found that NR/M(A&M) system has higher flame retardancy than that of NR/MCAPP/MCM-41. This enhancement in flame retardancy is thought to be due to the fact that when the NR composites containing M(A&M) were heated, MF resin as the inner shell of MCAPP released water vapor and NH_3 gases, which reduced the concentration of air and made the NR materials swell to form intumescent char [10]. This system with covalently anchored functional groups on the silica causes its surface to have specific attributes, such as a stereochemical configuration and binding sites that enhance compatibility with organic binders which improve thermal stability. That is the reason why NR/M(A&M) system has a relatively high LOI value compared with our previous double-layered microencapsulation with MF resin and ZB outside APP and MCM-41 [10].

Moreover, MCM-41 can reduce not only the amount of amorphous char protecting but also the intumescent char strengthening. The above results show that the presence of MF resin and OS outside APP and MCM-41 enabled M(A&M) to be an effective flame retardant in NR compared with APP/MCM-41. This enhancement in flame retardancy is thought to be due to the combined effect of higher char yield, physical dilution of the combustible gases through the decomposition processes of M(A&M), and the heat-sink effect of the synergist MCM-41.

Mechanical properties

Table 2 shows the mechanical properties of NR and FRNR composites. The tensile strength value and elongation at break were 6.62 MPa and 276.6 % for the NR/APP system, as well as 22.5 MPa and 452.6 % for NR, respectively. It is clear that addition of IFR filler had markedly decreased the mechanical properties of the composites. However, compared with un-microencapsulated samples, NR/M(A&M) system evidently increases the tensile strength and elongation at break. This finding was due to the fact that OS as the outer shell of double-shell microencapsulation is organic and can reinforce the strength of microencapsulation and the formation of M(A&M)-rubber coupling as shown in Fig. 5. Complications arise during mixing compounds as several chemical reactions tend to take place, such as silica and silane reaction, M(A&M)-rubber coupling and crosslinking between the rubber chain reaction. This kind of coupling or crosslinking makes the double-shell microcapsule get better dispersion within NR matrix and let NR/M(A&M) composites to achieve proper

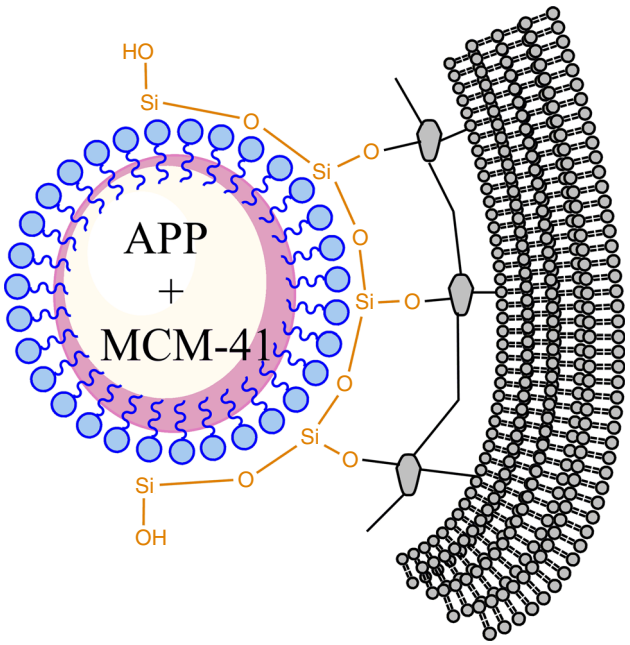

Fig. 5 Silica-silane-rubber coupling

mechanical properties. The tensile strength value and elongation at break are 8.23 MPa and 309.6 % for the NR/M(A&M) composites. On the other hand, these evident enhancements in tensile strength and elongation at break are likely to due to the synergist MCM-41, which results in the reinforcement of NR composites.

Morphology of burnt composites

As mentioned above, the residue of char plays a significant role in improving flame-retardant property of NR; thus, the investigation of combustion residues could help to understand the synergistic effect of the flame-retardant system. Figure 6 shows the SEM images of carbonaceous residues of burnt NR/APP (NRAPP), NR/MCAPP, NR/M(A&M), and NR/APP/MCM-41 after LOI test. As displaced in Fig. 6a, a relative loose structure, lot of cracks, cavities, and some incomplete hollow-fractured bubbles can be observed on the surface of the char residue in NR/APP. Consequently, heat and flammable volatiles can easily penetrate through the char layer into the interior of the composites during combustion. After being single-layered microencapsulated with MF resin, NR/MCAPP forms a relatively complete char layer that had fewer, smaller cracks and cavities than NR/APP. Regarding the NR/M(A&M) composite (Fig. 6c), the microstructure of the char residue displays a more compact structure and almost no cavities compared with signal-layered microencapsulated system (Fig. 6b). This finding indicates that double-layered microencapsulation is effective in forming a stronger char layer. The Si–O-Si network structure of double-shell microcapsule plays an important role in condensed phase. On one hand, silicon-containing compounds have good trapping ability of active free radicals in the vapor phase, leading to decreased smoke and materials. On the other hand, the char layer can be further strengthened by the strong ceramic network [19]. Furthermore, the synergist MCM-41 can effectively slow down the degradation of underlying materials and stop the transfer of heat and flammable volatiles. For NR/APP/MCM-41 (Fig. 6d), the char layer is non-uniformly inflated, but a compact structure is formed. The bigger inflated bubble can easily fracture. Analysis of these images suggests that the addition of MCM-41 and double-layered microencapsulation with MF resin and OS outside APP and MCM-41 positively affects the FR properties of NR composites.

Thermal stability

Figure 7 shows the TG curves of NR and FRNR composites. The related TG data are listed in Table 3. Thermal degradation of pure NR under N_2 atmosphere involved two steps, in which the thermal degradation takes place in the range of 220–470 °C, and steadily decomposed at 470 °C. In the presence of APP, the NR/APP system significantly decreased T20 % to 352.07 °C compared with pure NR; moreover, residue is improved. This improvement may be due to the fact that the decomposition of IFR took place in the first place, and then isolates NR from heat and oxygen to enter. The decomposition processes of NR/M(A&M) composite show T50 % of 421 °C, which is 27 and 21 °C higher than NR and NR/MCAPP, respectively. The degradation of NR/M(A&M) ends with a mass loss of 36.76 % higher than the other samples. The enhancement in the char residue at 600 °C is connected to the improvement in the anti-flammability of NR composites. This phenomenon may be due to the fact that the OS shell materials are advantageous to form carbonaceous-silicate charred layer building up on the surface, which insulates the core material and slows the escape of the volatile products generated during thermal degradation. The carbonaceous-silicate charred layers may create a physical protective barrier on the surface of the microencapsulated composites. This protective barrier can limit the transfer of flammable molecules to the gas phase, the transfer of heat from the flame to the condensed phase, and oxygen diffusion in the condensed phase [20]. On the other hand, MCM-41 dispersed in the composites shows good barrier properties and high thermal stability, which may slow down heat transmission to the polymer, consequently delaying the decomposition of the composites [21]. Therefore, the thermal stability of the NR/M(A&M) composite is remarkably better than those of the other samples.

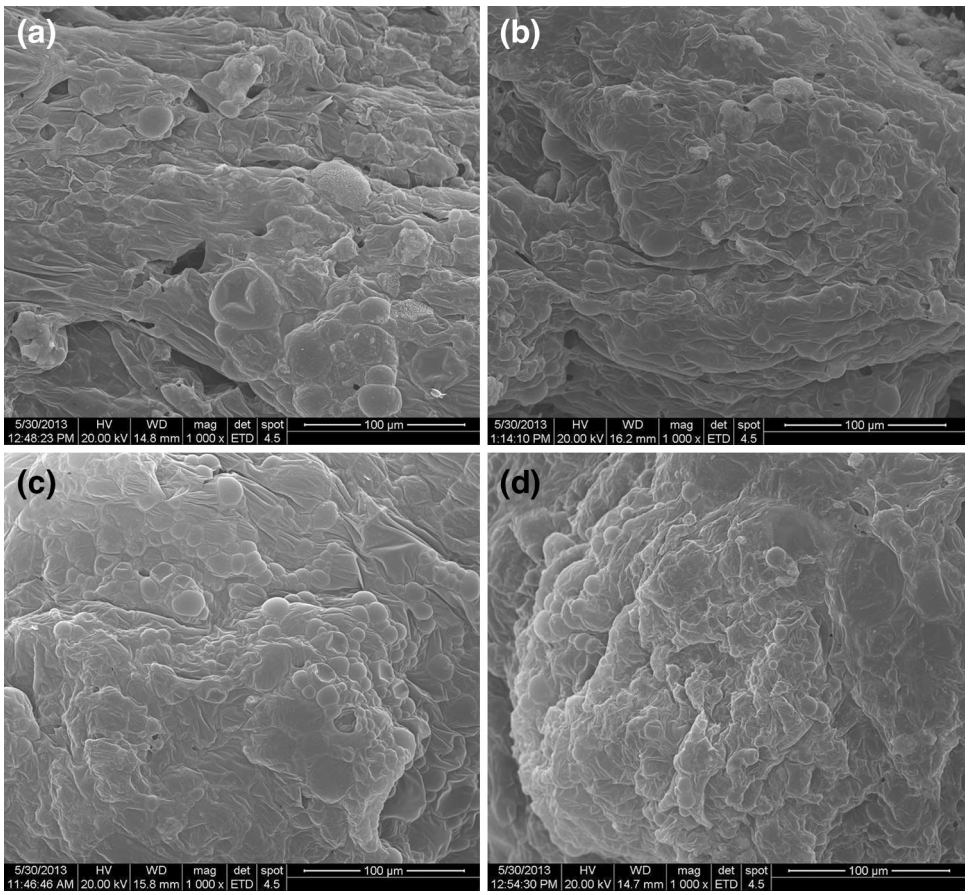

Fig. 6 SEM images of flame-retardant composites (1,000×): **a** NR/APP, **b** NR/MCAPP, **c** NR/M(A&M), and **d** NR/MCAPP/MCM-41

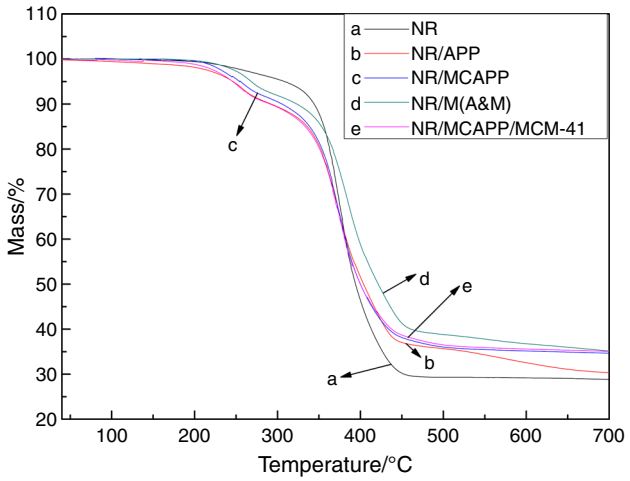

Fig. 7 TG curves of *a* NR, *b* NR/APP, *c* NR/MCAPP, *d* NR/M(A&M), and *e* NR/MCAPP/MCM-41

DMTA

Figures 8 and 9 depict the dynamic mechanical spectra (dynamic storage modulus and loss factor *tan* δ) as a function of temperature for the NR and FRNR composites. There is a remarkable increase in the storage modulus for

Table 3 TG data of flame-retardant NR composites

Sample	T20 %/°C[a]	T50 %/°C[b]	Char residue at W600/%
NR	362.61	394.06	29.18
NR/APP	352.07	403.77	32.54
NR/MCAPP	353.73	400.01	35.15
NR/M(A&M)	366.72	421.50	36.76
NR/MCAPP/MCM-41	350.84	399.79	35.58

[a] Temperature at 20 % mass loss/and

[b] Temperature at 50 % mass loss

NR/M(A&M) composites compared to other samples, which indicates that double-shell microencapsulation enhances the compatibility between the IFR and the matrix system. The glass transition temperature (T_g) of the samples determined from the temperature at the maximum *tan* δ is as follows: NR/APP (−51.82 °C), NR/MCAPP (−49.80 °C), NR/M(A&M) (−48.36 °C), and NR/APP/MCM-41 (−50.08 °C). In Fig. 9 the loss factor *tan* δ is shown for different vulcanizates. The maximum of *tan* δ peak reduces significantly suggesting a strong adhesion between NR and microencapsulation. Sliding along the intercalated interlayer is suppressed. In addition, MCM-41

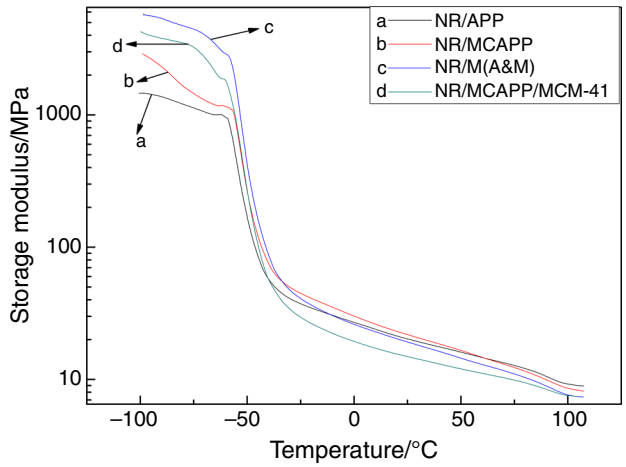

Fig. 8 Temperature dependence of *tan δ* of NR and FRNR composites: *a* NR/APP, *b* NR/MCAPP, *c* NR/M(A&M), and *d* NR/MCAPP/MCM-41

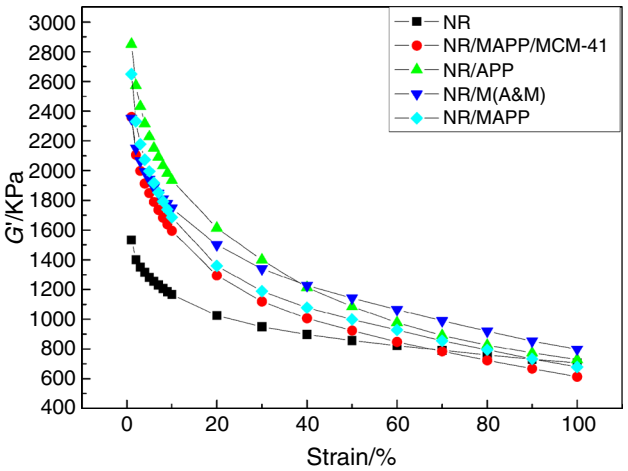

Fig. 10 Dependence of *G'* on strain of NR and FRNR compounds

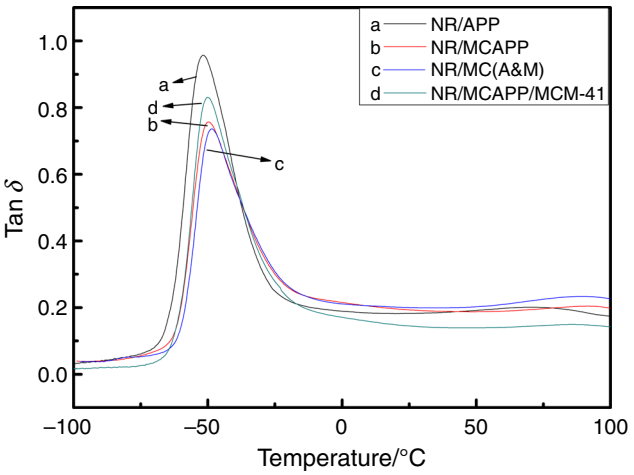

Fig. 9 Temperature dependence of storage modulus of NR and FRNR composites: *a* NR/APP, *b* NR/MCAPP, *c* NR/M(A&M), and *d* NR/MCAPP/MCM-41

with the NR matrix such as physical and chemical adsorption to reduce chain mobility, chain slipping at the outer surfaces of the aggregates is likely also hampered. Therefore, the loss maximum is the smallest in case of the system with the strongest filler matrix (NR/M(A&M)).

RPA

Figures 10 and Table 4 show the dependence of *G'* on strain of NR and FRNR composites to confirm the dispersion of fillers in the cured compounds. All the samples show a typical Payne effect. The *G'* decreases dramatically at strain 1 %, and *G'* almost reaches the same value as that of unfilled rubber at the ultimate strain of 100 %; *G'* is used to indicate the strength of the filler network [22].

Table 4 $\Delta G'$ values

Sample	$\Delta G'$/MPa
NR	0.827
NR/APP	1.552
NR/MCAPP	1.747
NR/M(A&M)	1.969
NR/MCAPP/MCM-41	2.122

The Payne effect of the compounds decreases in the order NR/APP (2.122 MPa) > NR/MCAPP(1.969 MPa) > NR/APP/MCM-41 (1.747 MPa) > NR/M(A&M) (1.552 MPa) > NR (0.827 MPa). Because the *G'* value decreases according to the reduced filler network strength [23], NR/M(A&M) has the best dispersion compared to other FRNR composites. Due to the existence of MCM-41, the dispersion of NR/APP/MCM-41 system is improved. This phenomenon may be due to the fact that the coupling or crosslinking between the OS shell materials and NR makes the double-shell microcapsule get better dispersed within NR matrix. Furthermore, the special channel structure of synergistic agent MCM-41 and its physical and chemical adsorption improve the dispersion of fillers.

Conclusions

Double-shell co-microencapsulated APP and mesoporous MCM-41 with MF resins and OS were successfully prepared by in situ polymerization. Due to the fact that the coupling or crosslinking between the OS shell materials and NR, the M(A&M) shows better compatibility in NR

system by the rubber process analyzer. Furthermore, MF resin and OS as the double shell of the microcapsules produce a synergism with IFR to form a mighty intumescent char; the result shows that NR/M(A&M) has a remarkable improvement in both mechanical properties and flame retardancy. A lowered *tan* δ peak value, an increased *Tg*, and the highest storage modulus are obtained in comparison with the other samples. When MCM-41 is added to the microcapsules, it effectively enhances the flame retardancy, mechanical, and thermal properties of NR composites by acting as a synergistic agent compared with the NR/MCAPP system. In summary, the NR/M(A&M) can be a promising formulation for FRNR composites.

Acknowledgements The Authors gratefully acknowledge the financial support of the National Natural Science Foundation of China (Grant No: 51103086, 51271188 and 51173110), State Key Lab of Organic–Inorganic Composites, Beijing University of Chemical Technology (201304), China Postdoctoral Science Foundation (grant No: 2012M510922), Program for Key Laboratory of Shenyang, China (Grant No: F11239100), Program for Economic and Information Commission of Liaoning Province, China (Grant No: 2012912).

References

1. Abdelmouleh M, Boufi S, Belgacem MN, Dufresne A. Short natural-fibre reinforced polyethylene and natural rubber composites: effect of silane coupling agents and fibres loading. Compos Sci Technol. 2007;67:1627–39.
2. Shen S, Yang M, Ran S, Xu F, Wang Z. Preparation and properties of natural rubber/palygorskite composites by co-coagulating rubber latex and clay aqueous suspension. J Polym Res. 2006;13:469–73.
3. Janowska G, Kucharska-Jastrząbek A, Rybiński P. Thermal stability, flammability and fire hazard of butadiene-acrylonitrile rubber nanocomposites. J Therm Anal Calorim. 2011;103:1039–46.
4. Janowska G, Kucharska-Jastrząbek A, Rybiński P, Wesołek D, Wójcik I. Flammability of diene rubbers. J Therm Anal Calorim. 2010;102:1043–9.
5. Wang BB, Wang XF, Tang G, Shi YQ, Hu WZ, Lu HD, Song L, Hu Y. Preparation of silane precursor microencapsulated intumescent flame retardant and its enhancement on the properties of ethylene–vinyl acetate copolymer cable. Compos Sci Technol. 2012;72:1042–8.
6. Wang N, Gao N, Jiang S, Fang QH, Chen EF. Effect of different structure MCM-41 fillers with PP-g-MA on mechanical and crystallization performances of polypropylene. Compos B. 2011;42:1571–7.
7. Chen X, Jiao C, Zhang J. Microencapsulation of ammonium polyphosphate with hydroxyl silicone oil and its flame retardance in thermoplastic polyurethane. J Therm Anal Calorim. 2011;104:1037–43.
8. Wu K, Wang ZZ, Hu Y. Microencapsulated ammonium polyphosphate with urea–melamine–formaldehyde shell: preparation, characterization, and its flame retardance in polypropylene. Polym Adv Technol. 2008;19:1118–25.
9. Wang N, Mi L, Wu YX, Wang XZ, Fang QH. Enhanced flame retardancy of natural rubber composite with addition of microencapsulated ammonium polyphosphate and MCM-41 fillers. Fire Safety J. 2013;62:281–8.
10. Wang N, Mi L, Wu YX, Zhang J, Fang QH. Double-layered comicroencapsulated ammonium polyphosphate and mesoporous MCM-41 in intumescent flame-retardant natural rubber composites. J Therm Anal Calorim. 2014;115:1173–81.
11. Dubois C, Rajabian M, Rodrigue D. Polymerization compounding of polyurethane-fumed silica composites. Polym Eng Sci. 2006;46:360–1.
12. Yan S, Yin J, Yang Y, Dai Z, Ma J, Chen X. Surface-grafted silica linked with l-lactic acid oligomer: a novel nanofiller to improve the performance of biodegradable poly (l-lactide). Polymer. 2007;48:1688–94.
13. Hsiao Shu C, Chiang HC, Chien-Chao Tsiang R, Liu TJ, Wu JJ. Synthesis of organic-inorganic hybrid polymeric nanocomposites for the hard coat application. J Appl Polym Sci. 2007;103:3985–93.
14. Bandyopadhyay A, De Sarkar M, Bhowmick AK. Epoxidised natural rubber/silica hybrid nanocomposites by sol-gel technique: Effect of reactants on the structure and the properties. J Mater Sci. 2005;40:53–62.
15. Wang N, Shao Y, Shi Z, Zhang J, Li H. Influence of MCM-41 particle on mechanical and morphological behavior of polypropylene. Mat Sci Eng, A. 2008;497:363–8.
16. Wang N, Shao Y, Shi Z, Zhang J, Li H. Preparation and characterization of epoxy composites filled with functionalized nanosized MCM-41 particles. J Mater Sci. 2008;43:3683–8.
17. Wu K, Wang Z, Hu Y. Microencapsulated ammonium polyphosphate with urea-melamine-formaldehyde shell: preparation, characterization, and its flame retardance in polypropylene. Polym Advan Technol. 2008;19:1118–25.
18. Fang G, Chen Z, Li H. Synthesis and properties of microencapsulated paraffin composites with SiO2 shell as thermal energy storage materials. Chem Eng J. 2010;163:154–9.
19. Qian Y, Wei P, Jiang P, Zhao X, Yu H. Synthesis of a novel hybrid synergistic flame retardant and its application in PP/IFR. Polym Degrad Stab. 2011;96:1134–40.
20. Zhang P, Hu Y, Song L, Lu H, Wang J, Liu Q. Synergistic effect of iron and intumescent flame retardant on shape-stabilized phase change material. Thermochim Acta. 2009;48:74–9.
21. Wang N, Yu S, Zhang J, Fang QH, Chen EF. Effect of nanosized mesoporous MCM-41 (with template) material on properties of natural rubber nanocomposites. Plast, Rubber Compos. 2011;40:402–6.
22. Robertson CG, Lin CJ, Bogoslovov RB, Rackaitis M, Sadhukhan P, Quinn JD, Roland CM. Flocculation, reinforcement, and glass transition effects in silica-filled styrene-butadiene rubber. Rubber Chem Technol. 2011;84:507–19.
23. Mihara S, Datta RN, Noordermeer JWM. Flocculation in silica reinforced rubber compounds. Rubber Chem Technol. 2009;82:524–40.